A descending dopamine pathway conserved from basal vertebrates to mammals

Dimitri Ryczko[a], Jackson J. Cone[b], Michael H. Alpert[c], Laurent Goetz[d], François Auclair[a], Catherine Dubé[a], Martin Parent[d], Mitchell F. Roitman[b], Simon Alford[c], and Réjean Dubuc[a,e,1]

[a]Groupe de Recherche sur le Système Nerveux Central, Département de Neurosciences, Université de Montréal, Montreal, QC, Canada H3C 3J7; [b]Department of Psychology, University of Illinois, Chicago, IL 60607; [c]Department of Biological Sciences, University of Illinois at Chicago, Chicago, IL 60607; [d]Department of Psychiatry and Neuroscience, Faculty of Medicine, Centre de Recherche de l'Institut Universitaire en Santé Mentale de Québec, Université Laval, Quebec, QC, Canada G1J 2G3; and [e]Département des Sciences de l'Activité Physique, Université du Québec à Montréal, Montreal, QC, Canada H3C 3P8

Edited by Sten Grillner, Karolinska Institute, Stockholm, Sweden, and approved March 15, 2016 (received for review January 14, 2016)

Dopamine neurons are classically known to modulate locomotion indirectly through ascending projections to the basal ganglia that project down to brainstem locomotor networks. Their loss in Parkinson's disease is devastating. In lampreys, we recently showed that brainstem networks also receive direct descending dopaminergic inputs that potentiate locomotor output. Here, we provide evidence that this descending dopaminergic pathway is conserved to higher vertebrates, including mammals. In salamanders, dopamine neurons projecting to the striatum or brainstem locomotor networks were partly intermingled. Stimulation of the dopaminergic region evoked dopamine release in brainstem locomotor networks and concurrent reticulospinal activity. In rats, some dopamine neurons projecting to the striatum also innervated the pedunculopontine nucleus, a known locomotor center, and stimulation of the dopaminergic region evoked pedunculopontine dopamine release in vivo. Finally, we found dopaminergic fibers in the human pedunculopontine nucleus. The conservation of a descending dopaminergic pathway across vertebrates warrants re-evaluating dopamine's role in locomotion.

motor system | brainstem | dopamine | conservation | Parkinson disease

Dopaminergic neurons represent a vital neuromodulatory component essential for vertebrate motor control, and their loss in neurodegenerative disease is devastating. The meso-diencephalic dopamine (DA) neurons are known to provide ascending projections to the basal ganglia, which, in turn, provide input to cortical structure in mammals but also project caudally to the mesencephalic locomotor region (MLR), a highly conserved structure that controls locomotion in all vertebrates investigated to date (1–7; for review, see ref. 8). A growing body of evidence supports the view that basal ganglia connectivity is highly conserved among vertebrates, from lampreys to mammals (9–11; for review, see ref. 12), with some interspecies differences recently highlighted (13). As such, the homology between DA cell populations remains to be resolved in vertebrates. As a general rule, DA neurons from the meso-diencephalon send projections to the striatum in all vertebrates. In lampreys and teleosts, those neurons are located only in the diencephalon (posterior tuberculum), but in tetrapods and cartilaginous fishes (14) they are located in both the diencephalon and the mesencephalon. An increasing number of authors seem to agree with the hypothesis that at least some of the meso-diencephalic DA neurons located in the diencephalon are homologous in all vertebrates, and thus, homologous to at least a portion of the mammalian substantia nigra pars compacta (SNc)/ventral tegmental area (VTA) (13, 15–19; for review, see ref. 20). Alternatively, it was suggested that the posterior tuberculum DA neurons projecting to the striatum in zebrafish are homologs of the mammalian DA neurons of the A11 group (21). This will be discussed below in light of the results of the present study.

In lampreys, only a few meso-diencephalic DA neurons send ascending projections to the striatum (9, 22); the majority of DA neurons send a direct descending projection to the MLR (22, 23), where DA is released and increases locomotor output through D1 receptors (22). These results demonstrate that the descending dopaminergic pathway to the MLR is an important modulator of locomotor output, but it remains to be determined whether this pathway is conserved in higher vertebrates.

The existence of a descending dopaminergic pathway that powerfully increases locomotor output has important implications for Parkinson's disease, which involves the meso-diencephalic DA neurons. A loss of descending dopaminergic projections could play a role in the locomotor deficits systematically observed in that disease. Because of the highly conserved nature of both the dopaminergic system and brainstem locomotor circuitry in vertebrates, we hypothesized that a direct descending dopaminergic pathway to the MLR also exists in higher vertebrates. Previous anatomical (24, 25) and electrophysiological (26) studies in rats support the idea of a descending connection from the SNc to the pedunculopontine nucleus [PPN, considered part of the MLR (2)]. Moreover, dopaminergic terminals were found in the PPN of monkeys (27), but the origin of this projection is still unknown in mammals.

Here, we investigated whether the direct descending projection from meso-diencephalic DA neurons to the MLR is present in two tetrapods, the salamander and the rat. Moreover, we supplement our analyses with anatomical data from human brain tissue. Using traditional and virogenetic axonal tracing, immunofluorescence, in vivo voltammetry, and calcium imaging of reticulospinal neurons,

Significance

In vertebrates, the contribution of dopamine neurons to locomotor control is traditionally attributed to their ascending projections to the basal ganglia that, in turn, project down to brainstem locomotor networks. We recently discovered in lampreys that brainstem networks receive a direct descending dopaminergic input that increases locomotor output. Here, we show that this descending dopaminergic pathway is conserved in higher vertebrates. We found that dopamine is released in salamander brainstem locomotor networks, together with reticulospinal cell activation, known to trigger locomotion. Dopamine is released in rat brainstem locomotor networks, and amphetamine potentiates dopamine release in vivo. Finally, brainstem locomotor networks in human tissue contain dopaminergic terminals. Our findings have important implications for understanding the locomotor role of dopamine in vertebrates.

Author contributions: D.R., F.A., and R.D. designed research; D.R., J.J.C., M.H.A., L.G., F.A., and C.D. performed research; D.R., J.J.C., M.H.A., L.G., F.A., C.D., M.P., M.F.R., S.A., and R.D. analyzed data; and D.R., F.A., and R.D. wrote the paper.

The authors declare no conflict of interest.

This article is a PNAS Direct Submission.

Freely available online through the PNAS open access option.

[1]To whom correspondence should be addressed. Email: rejean.dubuc@gmail.com.

This article contains supporting information online at www.pnas.org/lookup/suppl/doi:10.1073/pnas.1600684113/-/DCSupplemental.

we provide anatomical and functional evidence strongly supporting a conserved role for the descending projections of meso-diencephalic DA neurons in the regulation of brainstem locomotor networks across the vertebrate subphylum.

Results

Meso-Diencephalic DA Neurons Project Down to the MLR in Salamanders. In salamanders, the location of the MLR coincides with cholinergic cells of the laterodorsal tegmental nucleus (LDT) of the isthmic region (5, 7). We found tyrosine hydroxylase-positive (TH^+) catecholaminergic fibers and varicosities in close proximity to MLR cholinergic neurons ($n = 12$ preparations) (Fig. 1 *A–C*) and close to MLR neurons retrogradely labeled from the reticular formation ($n = 6$) (Fig. S1 *A–D*). Immunofluorescence experiments against DA ($n = 2$) showed that a large proportion of the catecholaminergic fibers in the MLR contained DA (Fig. S1 *E–G*). In one other preparation, DA^+ varicosities were confirmed to be present around the dendrites of MLR cells (Fig. 1 *D–G*) retrogradely labeled from the reticular formation. Tracer injections in the reticular formation were verified by histology (Fig. S2 *A–C*).

We then searched for the neurons at the origin of the dopaminergic innervation of the MLR using biocytin injections in the MLR (Fig. S2 *F–H*) coupled with TH ($n = 11$) or DA ($n = 2$) immunofluorescence. Labeling with TH or DA yielded very similar results (compare Fig. 1 *H–N* and Fig. S1 *H–N*). The whole brain and rostral spinal cord were scanned, and double-labeled neurons were found exclusively in the posterior tuberculum (PT), in the dorsomedial and ventrolateral portions. Neurons that were only immunoreactive for DA (circled areas in Fig. S1 *I* and *K*) and not for TH in our material (Fig. 1 *I* and *K*) were not labeled by the tracer injections. Such cells have been proposed to be putative DA-accumulating cells (28), but more recently, evidence seems to support that they rather express another form of TH not detected by currently available antibodies (29).

Next, the distribution of the meso-diencephalic DA neurons projecting to the MLR and to the striatum were compared using triple-labeling experiments ($n = 5$). In these preparations, biocytin was injected in the striatum (Fig. S2 *D* and *E*), Texas red-dextran amines (TRDA) in the MLR (Fig. S2*I*), and TH immunofluorescence was examined in the PT. DA neurons projecting to the striatum were mostly found in the mesencephalon and some were also observed in the dorsomedial portion of the PT, where they

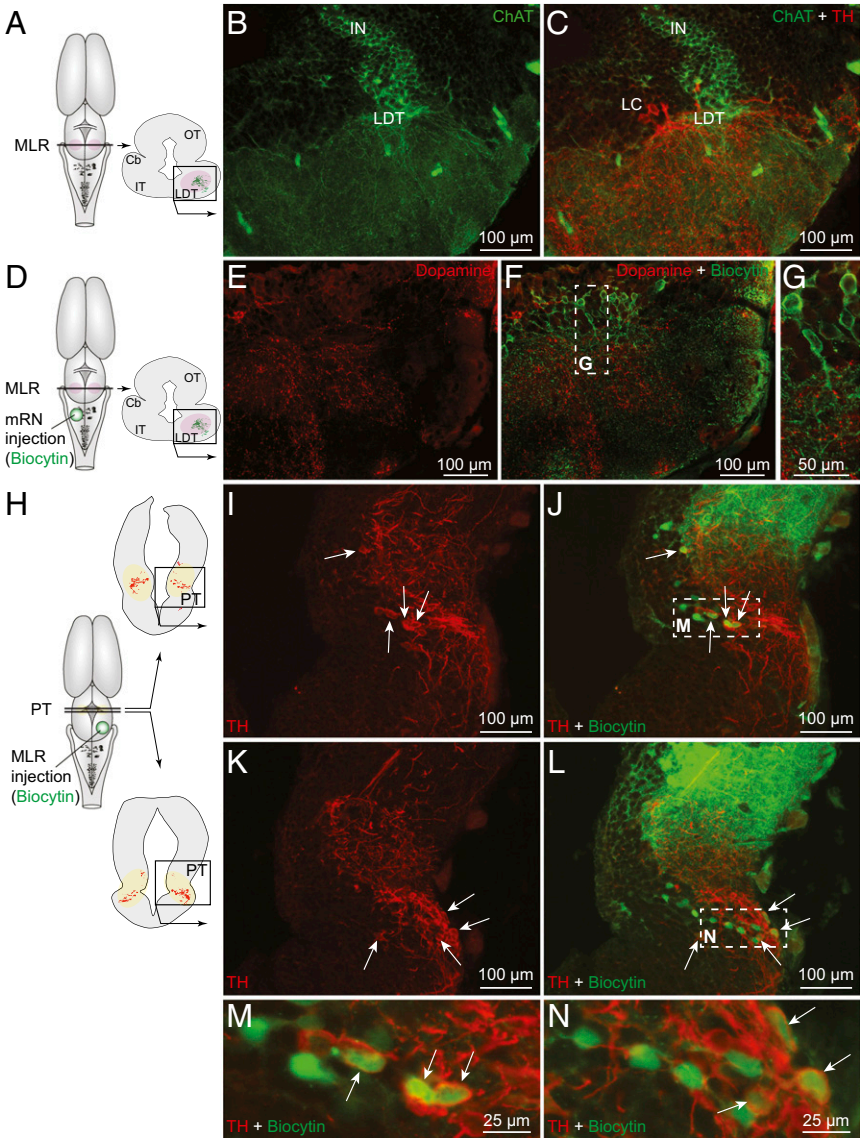

Fig. 1. DA cells from the PT project down to the MLR in salamanders. (*A*) Schematic dorsal view of the salamander brain. On the right, the diagram illustrates a cross section at the level of the MLR with the approximate location of the photomicrographs shown in *B* and *C*. (*B* and *C*) Fibers and varicosities immunoreactive to TH (red) in proximity with MLR cells positive for ChAT (green) in the LDT. Cell bodies of the locus coeruleus (LC) are also visible. (*D–G*) DA (red)-containing fibers and varicosities surrounded the dendritic fields of MLR cells retrogradely labeled from an injection of the tracer biocytin (green) in the mRN (Fig. S2*C*). (*G*) Magnification of the dashed rectangle in *F*. (*H–N*) Unilateral injection of the tracer biocytin (green) in the MLR (injection site; Fig. S2*G*) followed by immunofluorescence against TH (red) revealed double-labeled cells in the PT (arrows). (*M* and *N*) Magnifications of the dashed rectangles in *J* and *L*, respectively. Cb, cerebellum; IN, isthmic nucleus; IT, isthmic tegmentum; OT, optic tectum. Data from *B* and *C*, *E–G*, and *I–N* are from three different preparations.

intermingled anatomically with some of the DA neurons that projected to the MLR (Fig. 2). We found no evidence that meso-diencephalic DA neurons projected to both the striatum and the MLR in our material.

PT Stimulation Activates Brainstem Locomotor Circuits in Salamanders and Evokes DA Release in the MLR. Reticulospinal neurons convey brainstem locomotor commands to spinal locomotor networks. To monitor brainstem locomotor network activation, reticulospinal neurons were recorded using calcium imaging. Electrical stimulation (10-s train, 5 Hz, 1–7 μA, 2-ms pulses, $n = 7$ preparations) (Fig. 3 *A–C*) or chemical stimulation of the PT with local microinjections of 4.15–9.24 pmol of D-glutamate ($n = 4$ preparations) (Fig. 3*F*) elicited calcium responses in reticulospinal neurons, indicating that PT neurons activate brainstem locomotor circuits.

To determine whether PT activation releases DA in the MLR, changes in DA concentration were measured following PT stimulation using fast-scan cyclic voltammetry (Fig. 3*D*). Electrical stimulation of the PT (10-s train, 5 Hz, 15 μA, 2-ms pulses) or chemical activation of the PT with local microinjections of 0.26–17.8 pmol of D-glutamate evoked an increase of DA concentration in the MLR ($n = 7$ preparations) (Fig. 3 *D* and *E*).

Next, we examined whether DA release in the MLR was associated with the activation of brainstem locomotor circuits. A strong positive correlation was found between the increase of DA concentration in the MLR and the increase in calcium responses in reticulospinal neurons recorded during the same trials ($R = 0.97$; $P < 0.001$; $n = 19$ stimulations in four preparations) (Fig. 3*F*). Histology was used to verify the locations of the stimulation (Fig. S2 *J* and *K*) and recording sites (Fig. S2 *L* and *M*). Results from these experiments suggest that the PT could play a role in locomotor control through a descending dopaminergic projection to the MLR.

Meso-Diencephalic DA Neurons Project Down to the MLR in Rats. In rats as in basal vertebrates, the location of the MLR coincides with cholinergic cells of the PPN in the isthmic region (2, 6; for review, see ref. 8). Numerous TH^+ fibers were found in the PPN ($n = 7$ preparations) (Fig. 4 *A–E*) and many of those contained the DA active transporter (DAT), a marker of dopaminergic fibers. Many DAT^+ fibers were in close proximity to MLR cholinergic cells ($n = 3$ preparations) (Fig. S4), suggesting that DA neurons could directly modulate the activity of MLR neurons.

We asked whether this innervation originates from meso-diencephalic DA neurons by using an innovative virogenetic tracing approach. We used transgenic rats expressing Cre-recombinase under the control of a TH-promoter (TH-Cre rats) (30). The PPN of TH-Cre rats was injected with a virus encoding a floxed yellow fluorescent protein (EYFP; see *Materials and Methods*). We used an adeno-associated virus-5 (AAV5) serotype, shown to infect cell bodies via retrograde transport from terminal fields (31). Thus, viral particles at the injection site are picked up by axon terminals and retrogradely transported to the cell bodies. However, EYFP will be expressed only by Cre^+ (i.e., TH^+) neurons. Thus, this strategy can be used to retrogradely label TH^+ inputs to the PPN. Viral injections in the PPN (injection site: Fig. S5 *A* and *B*) retrogradely labeled numerous cells in the SNc (A9) and a few in the retrorubral field (RRF, A8) ($n = 3$) (Fig. 4 *F–J*). Interestingly, DA neurons of the VTA (A10) did not project to the PPN in our material. To ensure the viability of our retrograde labeling strategy, we also injected the EYFP virus into the striatum of a separate group of transgenic animals (Fig. S6 *A–C*). As expected, striatal viral injections labeled numerous cells in the SNc, RRF, and VTA (Fig. S6 *D–F*) ($n = 2$), which is consistent with the well-established anatomy of striatal dopaminergic inputs. In all cases in which the virus was injected, the retrogradely labeled neurons were confirmed to be TH^+ (Fig. 4 *H–J* and Fig. S6 *D–F*). The presence of the dopaminergic projection from the SNc/RRF to the MLR was confirmed by injecting traditional retrograde tracers into the PPN (Fast blue: $n = 2$; TRDA: $n = 6$) and examining TH immunofluorescence (Fig. 5*D*).

Next, the distribution of the meso-diencephalic DA neurons projecting to the MLR or to the striatum were compared using triple-labeling experiments ($n = 6$ preparations). The six animals injected in the PPN with TRDA (see above) were also injected in the striatum with Fast blue. A large number of the meso-diencephalic DA neurons that were first shown to project to the PPN also projected to the striatum (Fig. 5), resulting in many triple-labeled neurons in the SNc and RRF. We further found an indirect confirmation of the latter result when we looked back at the animals used for virogenetic tracing. Virus injections in the PPN led to $EYFP^+$ fibers in the striatum (Fig. S5 *C–F*) ($n = 2$ preparations), whereas virus injections in the striatum led to $EYFP^+$ fibers around choline acetyltransferase-positive ($ChAT^+$) cells in the PPN (Fig. S6 *G–I*) ($n = 2$ preparations). This finding indicates that the virus labels the whole neuron, including the axons that project to other targets in the brain. Again, all tracer injection sites in the striatum and PPN were histologically verified (Fig. S7). Taken together, these results indicate that many meso-diencephalic DA neurons not only send ascending projections to the basal ganglia, but also descending projections to the MLR in rats.

SNc/RRF Stimulation Evokes DA Release in the PPN in Rats. To determine whether the descending projections from SNc/RRF release DA in the MLR, we used fast-scan voltammetry in anesthetized rats. Changes in DA concentration in the PPN were measured following electrical stimulation of the SNc/RRF. Electrical stimulation of the SNc/RRF region (Fig. S8 *A* and *B*) evoked DA release (Fig. 6 *A* and *C*) ($n = 7$ preparations) around $ChAT^+$ neurons of the PPN (Fig. S8 *C–E*). Given the well-known increase in locomotor activity induced by psychostimulants, we hypothesized that the descending dopaminergic pathway could be a relevant target for such drugs. We next tested whether the PPN dopaminergic signal was sensitive to amphetamine. Notably, amphetamine (5 mg/kg, injected intraperitoneally) significantly potentiated the DA release evoked in the PPN by SNc/RRF stimulation (+172 ± 58% on the response area vs. baseline, $P < 0.05$, paired t test; $n = 6$ preparations) (Fig. 6 *B–D*). This finding indicates that amphetamine increases in vivo the direct dopaminergic drive from the SNc/RRF to brainstem locomotor networks.

The Human PPN Is Innervated by Dopaminergic Fibers. We then examined whether evidence for a dopaminergic innervation of the PPN was also present in a human brain ($n = 1$), using double-immunofluorescence experiments. Much like in salamanders and rodents, TH^+ fibers were found in close proximity to $ChAT^+$ cells in the PPN (Fig. S9). At least part of this innervation was dopaminergic, because fibers positive for DAT were present near $ChAT^+$ cells in the PPN (Fig. 7). This finding indicates that a dopaminergic projection could modulate a known component of the MLR in the human brainstem.

Discussion

Our results provide anatomical and functional evidence supporting a conserved role for the descending projections of meso-diencephalic DA neurons in regulating brainstem locomotor networks from basal vertebrates to mammals. We show in amphibians and mammals that descending projections from these DA neurons support DA release in the MLR. We demonstrate that DA release in the MLR is associated with the activation of brainstem locomotor networks. We also show that DA release in the MLR is increased in vivo by amphetamine, a psychostimulant that is known to increase locomotor activity by enhancing extracellular DA concentrations. Finally, we provide evidence for a dopaminergic innervation of the human MLR. The ascending

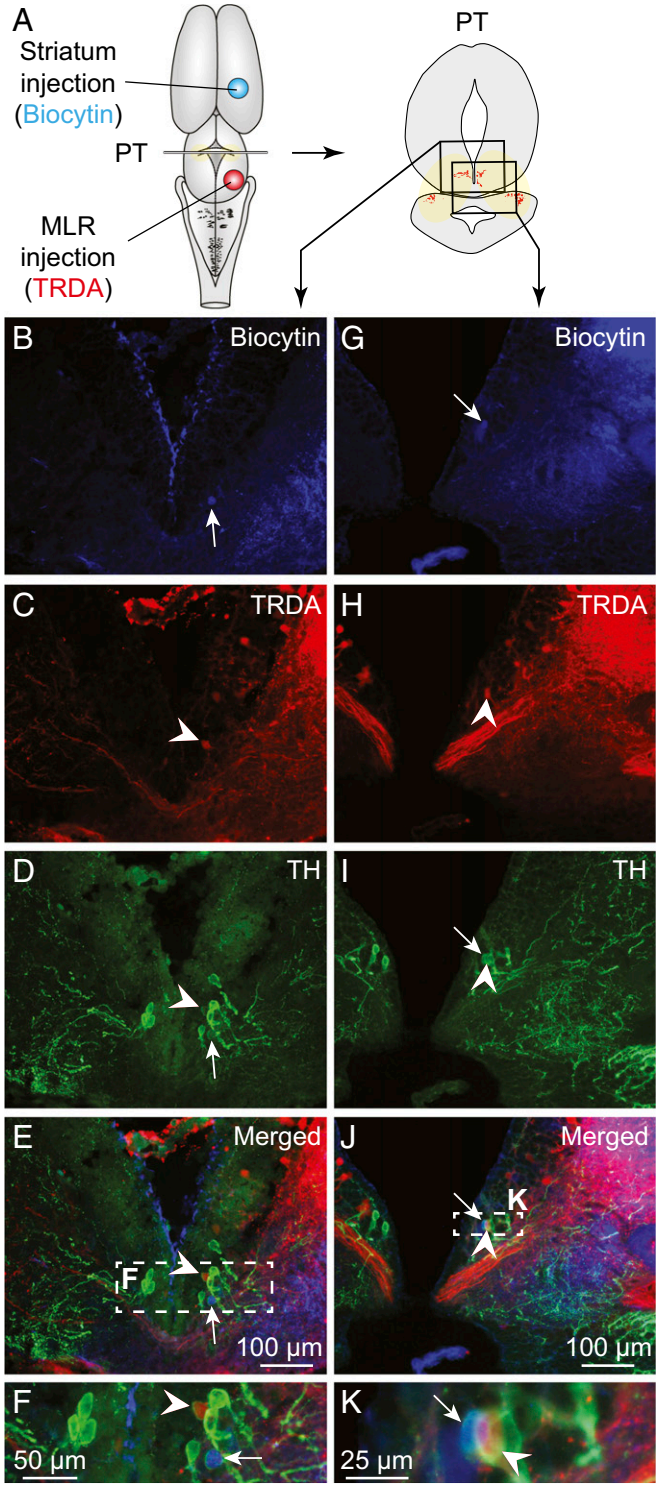

Fig. 2. TH$^+$ cells projecting to the MLR or to the striatum are intermingled in the PT. (*A*) Schematic dorsal view of the salamander brain, with the approximate location of the tracer injection sites in the striatum (biocytin, blue) and in the MLR (TRDA, red) (injection sites in Fig. S2 *E* and *I*, respectively). (*Right*) A diagram illustrates a PT cross section with the approximate location of the photomicrographs shown in *B*–*E* and *G*–*J*, obtained following triple-labeling experiments performed in two different animals. (*B* and *G*) Unilateral injection of a tracer in the striatum- (biocytin, blue) labeled cells in the PT. (*C* and *H*) Unilateral injection of another tracer in the MLR (TRDA, red) also labeled cells in the PT. (*D* and *I*) DA neurons of the PT were identified using immunofluorescence against TH (green). (*E*, *J*, *F*, and *K*) The photomicrographs were merged to show the three markers. Arrowheads indicate examples of TH$^+$ cells of the PT that project to the MLR. White arrows point to TH$^+$ cells projecting to the striatum. (*F* and *K*) Magnifications of the dashed rectangles in *E* and *J*, respectively.

projections from DA neurons are well-known to be important for planning movements in physiological and pathological conditions (e.g., ref. 11). However, several anatomical studies have reported the existence of a descending projection from the SNc to brainstem locomotor networks in mammals (24, 25, 32, 33), and this was further supported by electrophysiological recordings (26). Few authors, however, have considered that this descending projection could originate from meso-diencephalic DA neurons (25). After showing the existence of a descending dopaminergic pathway and its role in locomotor control in lampreys (22), we now present evidence that this pathway is strongly conserved across the vertebrate subphylum, perhaps even in humans. Therefore, our results have broad implications for the role of DA in locomotion and suggest that loss of the dopaminergic innervation of the MLR could contribute to the locomotor deficits seen in patients with Parkinson's disease.

A Conserved Innervation of the MLR by Meso-Diencephalic DA Neurons. The functional projection of dopaminergic neurons to the MLR is likely to be critically important to the outcome of descending motor commands in activating and maintaining locomotion. The MLR controls vertebrate locomotor speed and mode and was first defined functionally in cats (1). Since then, its function has been confirmed in all vertebrates tested, from lampreys and salamanders, to birds, rats, cats, and monkeys (8). In humans, locomotion is impaired when the MLR is damaged (34, 35). The location of effective MLR stimulation sites was consistently found to coincide with the location of cholinergic neurons (2, 5, 35, 36; for review, see ref. 8). Based on this, we examined the dopaminergic innervation of isthmic cholinergic neurons, while being aware that neurons expressing other neurotransmitters in this region are also part of the MLR [e.g., MLR glutamatergic neurons in lampreys (37), salamanders (7), and mice (38)].

Our results demonstrate that the MLR receives an input from meso-diencephalic DA neurons in salamanders and rats, which supports DA release within the MLR. This finding is consistent with a report in monkeys, where a third of the DAT$^+$ fibers in the PPN also contained the synaptic marker synaptophysin (27), indicating local synaptic output; although we do not have direct physiological evidence for this descending pathway in humans, the presence of dopaminergic terminals in the human MLR suggests it is present.

Our data show that in both species, DA is released in the MLR after stimulation of the region containing meso-diencephalic DA neurons. Electrical stimulation not only activates cell bodies but also axons of passage. In some experiments in salamanders, we used chemical stimulation to circumvent the effect of activating *en passant* fibers, and the results were the same, as previously reported with similar control experiments in lampreys (22). We are thus confident that DA release in the MLR of rats is also evoked by the recruitment of dopaminergic cell bodies in the SNc and RRF, even though only electrical stimulation was used. Importantly, we found that the time-scale of DA release in the MLR was highly correlated with the activation of brainstem locomotor networks, as previously reported in lampreys (22).

Comparative Aspects. In salamanders, our results confirm those of previous studies showing that the meso-diencephalic DA neurons span from the mesencephalic oculomotor nucleus to the diencephalon (28, 39). Our results also confirm that the DA neurons that project to the striatum are mostly located in the mesencephalon (15). We also show that the DA neurons that project to the MLR are largely located in the diencephalon. The

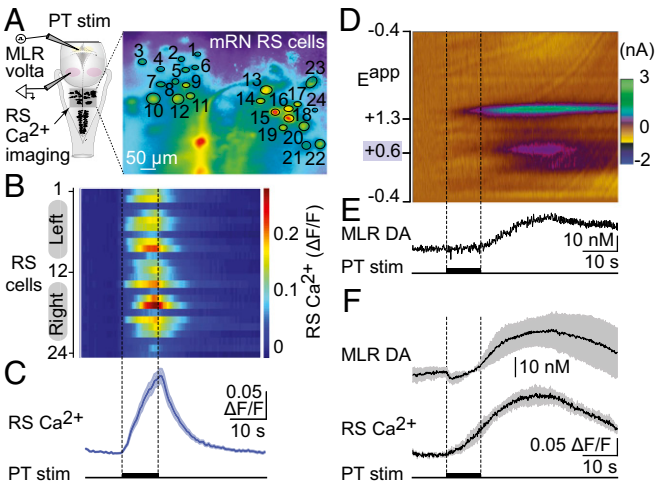

Fig. 3. Stimulation of the PT evokes DA release in the MLR together with RS activity in salamanders. (*A*) Schematic dorsal view of the salamander brain. (*Right*) Ca^{2+} fluorescence at rest of RS cells (encircled in black) of the mRN labeled with Ca^{2+} Green dextran amines. (*B*) Color plots illustrating the Ca^{2+} responses (ΔF/F) of RS cells in response to PT stimulation (10-s train, 5 Hz, 2.5 µA, 2-ms pulses) (Fig. S2 *J–K*). Each line illustrates the response of individual cells that are numbered from top to bottom: cells 1–12 located on the left side of the brain and cells 13–24 on the right side. Warmer colors (red) indicate larger Ca^{2+} responses. (*C*) Average Ca^{2+} response for the 24 cells illustrated in *A* and *B*. (*D*) Local activation of cell bodies in the PT by microinjections (10-s train, 2 Hz, 50-ms pulses) of D-glutamate (5 mM, 2 Hz, 20 pulses of 50–200 ms, 5–20 psi, 0.05–3.57 nL per injection) evokes DA release in the MLR (Fig. S2 *L* and *M*). Single-trial color plot depicts current changes (color) as a function of electrode potential (*y* axis) across time (*x* axis). DA [identified by its oxidation (~0.6 V; purple feature) (Fig. S3*B*)] was transiently evoked following PT activation. We detected an additional electroactive species (~1.2 V, green feature) that we identified as hydrogen peroxide (Fig. S3 *A* and *B*). (*E*) Changes in DA concentration in the MLR extracted from the electrochemical data in *D*. (*F*) Average simultaneous change in MLR DA concentration and RS Ca^{2+} responses in the same trials ($n = 19$ stimulations from four preparations) in response to chemical stimulation of the PT with D-glutamate (5 mM, 2 Hz, 20 pulses of 100–200 ms, 10 psi, 0.83–1.85 nL per injection). Mean ± SEM are illustrated.

two populations overlap slightly at the transition from mesencephalon to diencephalon. In our material, no neurons were found to project to both the striatum and the MLR in salamanders. However, we cannot exclude the possibility that such neurons exist in very rare cases. In lampreys, neurons projecting to both the striatum and the MLR were very rare (22). In contrast, in rats, one remarkable aspect of our findings is that the vast majority of the DA neurons that project to the striatum also project to the MLR, implying a simultaneous ascending and descending modulation of the entire locomotor command circuitry from cortex to brainstem. These DA neurons are mostly located in the SNc with a few in the RRF, two structures that are classically considered as mesencephalic but that also span in the diencephalon (16, 19, 20). In lampreys, the terminology "mesodiencephalic DA neurons" does not apply, given that the DA neurons are all located in the diencephalon (40). The neurons from this DA population that project to the MLR and to the striatum are highly intermingled in lampreys, with very rare neurons projecting to both structures. One can only speculate as to why striatum-projecting and MLR-projecting DA neurons are mostly segregated in two different populations in lampreys and salamanders, although it seems that only one population of DA neurons innervates both structures in the rat. Fig. S10 provides a comparison of the ascending and descending projections of diencephalic and mesencephalic DA neurons in lampreys, salamanders, and rats.

When comparing ascending vs. descending projections of meso-diencephalic DA neurons in lampreys, salamanders, and rats, it appears that the proportion of ascending projections increases during evolution. This may result from growing demands caused by the expansion of the basal ganglia in mammals vs. basal vertebrates (for review, see ref. 12). One other interesting observation is that no neurons in the VTA (A10) were found to project to the MLR in rats. This finding suggests that the DA neurons that do project to the MLR in the SNc (A9) are homologs of the DA neurons that project to the MLR in more basal vertebrates, whereas the VTA could either have a phylogenetically more recent origin or could contain neurons homologous to DA neurons in lampreys and salamanders that only project to the striatum.

Another group of DA neurons, located in the hypothalamus (A11), sends descending projections to the spinal cord in lamprey (41), zebrafish (42), mice (43), rats (44), and primates (45). Altogether, our results from lamprey to human (ref. 22 and present study) indicate that A11 neurons are not responsible for

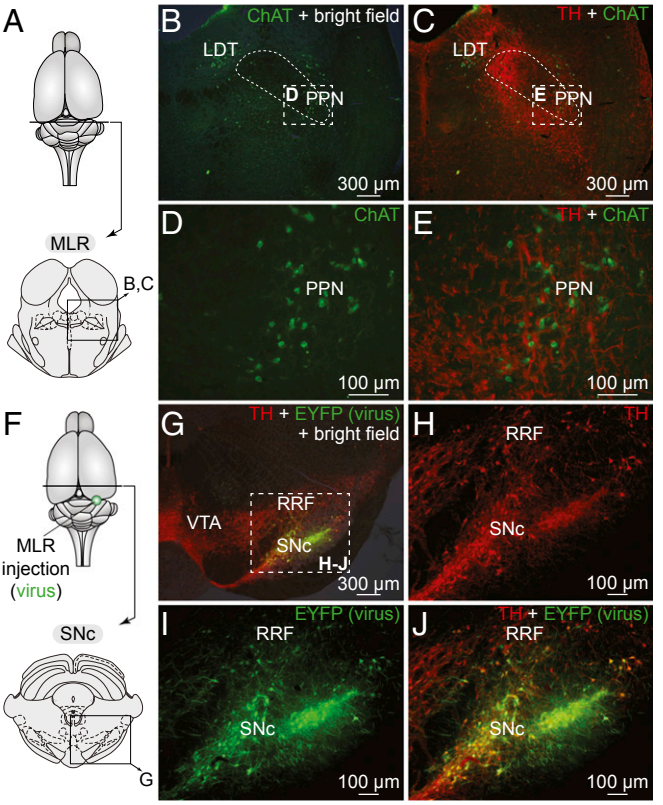

Fig. 4. DA cells from the SNc project down to the MLR in rats. (*A*) Schematic dorsal view of the rat brain. At the bottom, the diagram illustrates a cross section at the level of the MLR with the approximate location of the photomicrographs shown in *B* and *C*. (*B–E*) Fibers and varicosities immunoreactive to TH (red) in proximity with cells positive for ChAT (green) in the PPN, a landmark of the MLR (2). (*D* and *E*) Magnifications of the dashed rectangles in *B* and *C*, respectively. In *B* and *C* the superior cerebellar peduncle is delineated with thin dashed lines. (*F*) Approximate location of the in vivo virus injection for virogenetic labeling experiments. At the bottom, the diagram illustrates a cross-section at the level of the SNc with the approximate location of the photomicrographs shown in *G*. (*G–J*) Cells retrogradely labeled in the SNc and to a lower extent in the RRF following injection in the PPN (Fig. S5 *A* and *B*) of a Cre-dependent virus encoding for the EYFP (green) in transgenic rats expressing Cre-recombinase in TH neurons. The cells labeled by this virus (green, *I*) were positive for TH (red, *H* and *J*) as previously reported (30). (*H–J*) Magnifications of the dashed rectangle in *G*. Data from *A–E* and *F–J* are from two different animals.

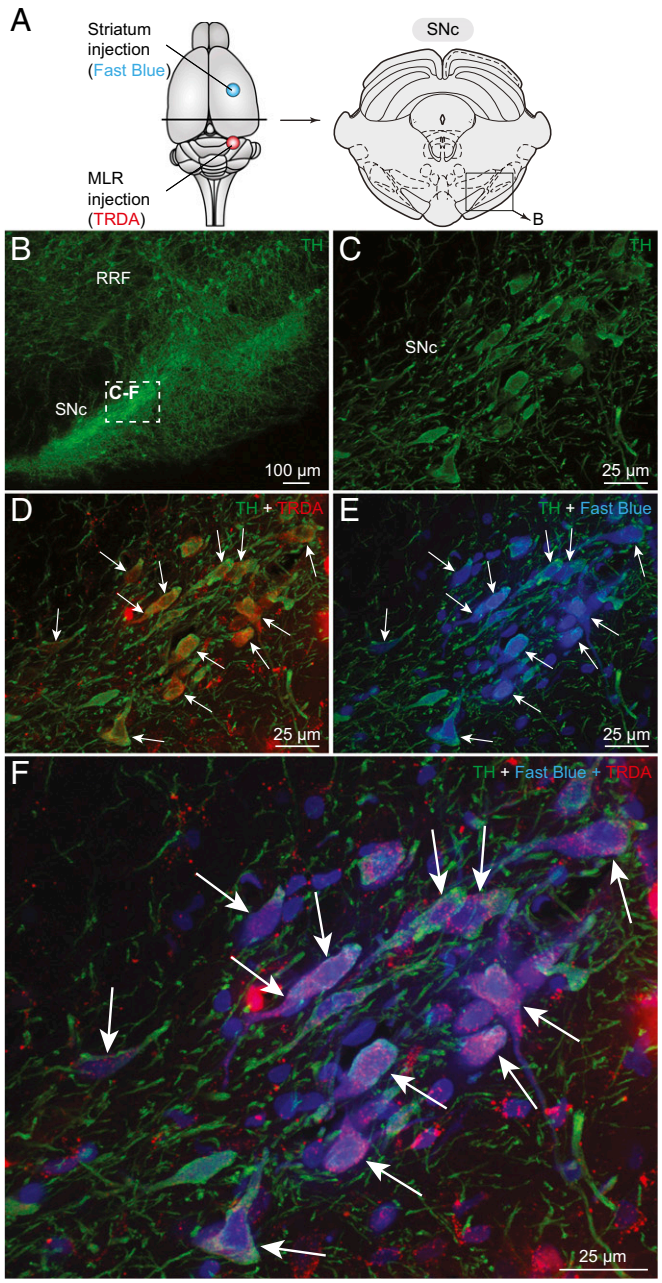

Fig. 5. TH neurons projecting to the striatum and to the MLR are intermingled in the SNc. (*A*) Schematic dorsal view of the rat brain with the approximate location of the tracer injection sites in the striatum (Fast blue, blue) and in the pedunculopontine nucleus (TRDA, red). (*Right*) Diagram illustrating a cross-section at the level of the SNc with the approximate location of the photomicrographs shown in *B*. (*B* and *C*) DA neurons of the SNc were identified using immunofluorescence against TH (green). (*B*) A magnification of the rectangle in *A*. (*D*) Injection of a tracer in the MLR- (TRDA, red) (Fig. S7 *C* and *D*) labeled numerous TH^+ cells (green) in the SNc. (*E*) Injection of another tracer in the striatum (Fast blue, blue) (Fig. S7 *A* and *B*) also labeled TH^+ cells (green) in the SNc. (*F*) The photomicrographs were merged to show the three markers. In *D*–*F*; the arrows indicate numerous examples of TH^+ cells of the SNc that project to the MLR and to the striatum. (*C*–*F*) Magnifications of the dashed rectangle in *B*.

the dopaminergic innervation of the MLR. In lampreys, the diencephalic DA neurons projecting to the spinal cord, which may correspond to the A11 group, are periventricular cells of the mammillary area (41) and are distinct from those projecting to the MLR and striatum (22). In rats, we did not find cells labeled in A11 following tracer or virus injection in the MLR. Importantly, A11 DA neurons do not express DAT in rats (46), primates (45), and humans (47), thus confirming that the DAT^+ innervation of the MLR that we report here in rats and humans does not originate from A11. However, the diencephalo-spinal dopaminergic projection originating from A11 could play a role in locomotor control (for review, see ref. 48). Interestingly, there is evidence that DA modulates spinal locomotor circuits. L-DOPA has been widely used to elicit stepping in spinalized cats. DA is released in the spinal cord during locomotion in rats (49), and in vitro application of DA on the spinal cord exerts opposite, concentration-dependent effects on locomotor output (for review, see ref. 48). The possible involvement of the descending dopaminergic projections from A11 in the control of spinal locomotor circuits remains to be determined.

Functional Significance. The conservation of the descending projection from the meso-diencephalic DA neurons to the MLR in vertebrates brings about new and important questions relative to the role of DA in locomotor control. We now show that this pathway is present and can release DA in the MLR of salamanders and rats, and perhaps humans. In lampreys and salamanders, DA release in the MLR is concurrent with the activation of reticulospinal neurons, which trigger locomotion by transmitting the locomotor command caudally to spinal locomotor networks. In lampreys, the PT sends direct descending dopaminergic and glutamatergic inputs to the MLR (22, 50). Importantly, in lampreys, pharmacological blockade of D1 receptors in the MLR dramatically decreased the duration of locomotor bouts, locomotor frequency, and the number of locomotor cycles elicited by PT stimulation (22). These effects were associated with a much weaker activation of brainstem locomotor networks. Taken together, these data suggest that the glutamatergic drive from the PT to the MLR is potentiated by the dopaminergic inputs, which leads to increased excitation of MLR neurons and an increase in locomotor output. There is evidence in the literature suggesting that interactions between these neurotransmitters also exist in mammals, where it was shown that glutamate colocalizes with DA in the SNc, VTA, and

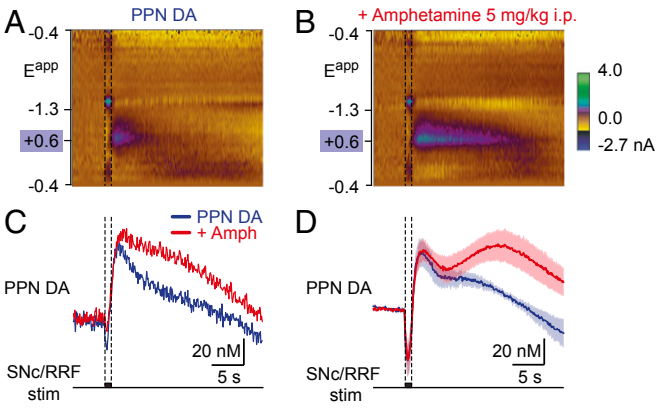

Fig. 6. Stimulation of the SNc/ RRF region evokes DA release in the PPN in vivo in rats. (*A* and *B*) DA release evoked in the PPN (Fig. S8 *C*–*E*) by electrical stimulation (1-s train, 60 Hz, 120 μA, 5-ms pulses) of the SNc/RRF region (Fig. S8 *A* and *B*) in urethane (1.5 g/kg) anesthetized rats. Single-trial color plot depicts current changes (color) as a function of electrode potential (*y* axis) across time (*x* axis). DA [identified by its oxidation (~0.6 V; green/purple feature) (Fig. S3*C*)] was transiently evoked following SNc/RRF stimulation. Control condition (*A*) and 20 min after intraperitoneal injection of amphetamine (5 mg/kg) (*B*). (*C*) Changes in DA concentration in control (blue) and following amphetamine injection (red) extracted from *A* and *B*. (*D*) Average DA concentration evoked in six preparations before (blue) and during the 15–85 min following amphetamine injection (red) ($n = 43$ stimulations in control and $n = 59$ stimulations following amphetamine). Mean ± SEM are illustrated.

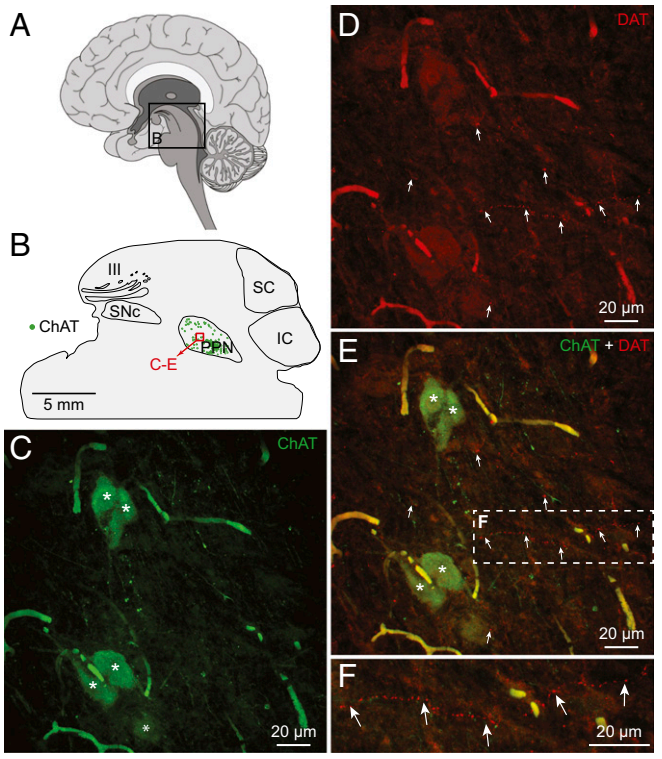

Fig. 7. Dopaminergic innervation of the MLR in the human brain. (*A*) Schematic sagittal view of a human brain illustrating the approximate location of the brain section at the level of the PPN, considered part of the MLR (35). (*B*) Schematic sagittal view of the brain section (laterality: 5.8 mm from midline) used for the illustrated immunofluorescence experiment. The location of PPN cells positive for ChAT (green) is illustrated. The approximate location of the photomicrographs in *C*–*F* is shown by a red square. (*C*–*F*) Fibers and varicosities containing the DAT (red, highlighted by arrows) in proximity with cholinergic cells (ChAT, green) in the PPN. (*F*) A magnification of the dashed rectangle in *E*. The images in *C*–*F* were obtained by projecting on the same plane a stack of 20 images (0.96-µm deepness per image) acquired along the *z* axis. Asterisks illustrate cholinergic cells bodies.

RRF (for review, see ref. 51). As demonstrated in the basal ganglia and cortex of mammals, we suggest that D1 receptor activation increases AMPA- and NMDA-mediated responses (52, 53) in MLR cells. D2 receptor activation is also not excluded. In the basal ganglia of mammals, the activation of D2 receptors decreases both AMPA- and NMDA-mediated components of glutamatergic responses (52, 53). Future work will determine whether DA and glutamate cooperate pre- and postsynaptically, and whether dopaminergic inputs act on intrinsic properties of MLR cells.

We propose that direct dopaminergic projections to the brainstem are activated in synchrony to ascending projections to the basal ganglia and are both involved in modulating locomotor output in parallel. The respective roles of the ascending versus descending projections of meso-diencephalic DA neurons in locomotor control remain to be characterized. Our present results show that the descending dopaminergic pathway likely plays a key role in the initiation and maintenance of locomotion in higher vertebrates. This is particularly interesting because the contribution of DA to locomotor control in vertebrates has traditionally been attributed to the ascending dopaminergic projections from the SNc/VTA to the basal ganglia, which in turn project down to the MLR. Furthermore, we demonstrate in rats that DA release in the MLR is potentiated by amphetamine in vivo; this strongly suggests an involvement of the descending dopaminergic pathway in the well-characterized increased locomotor activity elicited by psychostimulants, as well as other dopaminergic drugs targeting meso-diencephalic DA neurons (e.g., L-DOPA). We propose that, whereas the ascending pathway is involved in the selection of motor actions through basal ganglia loops, the direct descending pathway is involved in controlling the excitability of brainstem motor circuits. Whether this pathway is also involved in other motor behaviors, for example the increased exploratory behavior elicited by novelty, to which many DA neurons respond (for review, see ref. 54), remains to be determined.

Finally, our findings may have implications for our understanding of the locomotor role played by DA in pathological conditions. It is well established in patients with Parkinson's disease that DA neurons of the SNc undergo degeneration. A depletion of the ascending dopaminergic input to the striatum is classically considered to be the main cause of motor deficits associated with the disease (e.g., ref. 11), particularly the inability of patients to initiate locomotion. However, the descending dopaminergic projection to the MLR we now describe will also be affected by the disease. Interestingly, a depletion of dopaminergic terminals was shown in the MLR of monkeys treated with MPTP (27), a neurotoxin used widely to cause the death of DA neurons of the SNc and to mimic symptoms of Parkinson's disease. The locomotor deficits in these pathological conditions may thus result, at least in part, from the loss of the descending dopaminergic inputs to the MLR and a consequent loss of amplification of descending locomotor commands.

A descending dopaminergic pathway is important for initiating and maintaining locomotor movements in basal vertebrates (22). We now show that such a pathway is also present and functional in higher vertebrates, and most likely in humans. The role of DA in locomotor control should be re-evaluated by taking into account the descending projections from meso-diencephalic DA neurons.

Materials and Methods

All procedures conformed to the guidelines of the Canadian Council on Animal Care and National Institutes for Health Guide for the Care and Use of Laboratory Animals, and were approved by the Animal Care and Use Committee at Université de Montréal, Université du Québec à Montréal, and University of Illinois at Chicago. Care was taken to minimize the number of animals used and their suffering. The human postmortem brain tissues were obtained from the Centre Universitaire en Santé Mentale de Québec. Informed consent was obtained from donors and the Ethics Committee at Institut Universitaire en Santé Mentale du Québec approved the collection, storage, and handling procedures.

Subjects. Thirty-two juvenile salamanders (*Notophthalmus viridescens*) of either sex (snout-vent length: 40–50 mm) were purchased from Connecticut Valley Biological Supply or Boreal Science and kept at 20 °C in fish tanks with aerated water and fed weekly with frozen bloodworms.

Seventeen male Sprague–Dawley rats (*Rattus norvegicus*; Charles River), and five female transgenic rats (Long-Evans background) expressing Cre recombinase under the control of a TH promoter (TH-Cre$^+$ rats) (30, 55) were used. All rats weighed between 300 and 400 g at the time of use. Rats were housed with ad libitum access to water and food in individual cages with lights on from 7:00 AM to 7:00 PM.

The human material came from one female without a known history of neurological disorder, who died of drug overdose at 68 y of age.

Surgical Procedures. Salamanders were anesthetized by immersion in an aqueous solution of tricaine methanesulphonate (MS-222, Sigma-Aldrich E10521; 200 mg/L) and transferred into Ringer's solution (8–10 °C, 100% O_2, pH 7.4: 130 mM NaCl, 2.1 mM KCl, 2.6 mM $CaCl_2$, 1.8 mM $MgCl_2$, 4 mM Hepes, 4 mM dextrose, and 1 mM $NaHCO_3$). After decapitation, the tissue around the cranium was removed and the brain and first spinal segments were exposed dorsally.

Rats were anesthetized with ketamine/xylazine (100/10 mg/kg, i.p.) for tracer injections, or with urethane (1.5 g/kg in 0.9% saline, intraperitoneally) for voltammetry experiments, and placed in stereotaxic frame (Kopf Instruments). A skin incision was made to reveal the skull. Following clearance of the fascia, small holes were drilled in the skull over the target regions. Brain coordinates for electrode placement, and tracer and virus injections were selected from the rat brain atlas of Paxinos and Watson (56).

The human tissue was collected 12-h postmortem. The brainstem was sliced midsagittally, fixed by immersion for 7 d at 4 °C in 4% (wt/vol) paraformaldehyde in 0.1 M phosphate buffer (pH 7.4, PB), and transferred in PB containing 0.9%

NaCl (pH 7.4, PBS) with 15% (wt/vol) sucrose and 0.1% sodium azide. The sections were then cut using a freezing microtome (Leica) into 50-μm-thick parasagittal sections collected in PBS until processing.

Anatomical Tracing and Histology in Salamanders. The procedure was similar to that previously used in lampreys (22, 57, 58) and salamanders (7). Biocytin (Sigma-Aldrich B-4261) and TRDA (Molecular Probes D-3328) were used for retrograde tracing. For tracer injections, a pulled glass micropipette was used to cut axons at the injection site and crystals of the tracers were placed in the lesion, allowing the tracer to be picked up by cut axons. After 10 min, the brain was rinsed thoroughly and transferred to a chamber perfused with oxygenated Ringer's solution for 3–4 h at room temperature to allow retrograde transport of the tracers. The injection sites were chosen based on previous studies on the MLR (5, 7, 59), middle reticular nucleus (mRN) (7, 60, 61), and striatum (15, 62) and verified by histology. The preparations were then transferred to a fixative solution according to the immunofluorescence procedure to follow. For TH and ChAT, the whole brain was immersed for 24 h in 4% (wt/vol) paraformaldehyde in PBS and then transferred to PB containing 20% (wt/vol) sucrose. For DA, the brain was immersed for 5 min in 0.1 M cacodylate buffer containing 0.9% sodium metabisulfite (MBS, pH 6.2), followed by 55 min in the same buffer with the addition of 2% (vol/vol) glutaraldehyde (pH 7.5). The tissue was then transferred overnight to 0.05 M Tris containing 0.9% MBS (TBMBS) and 20% (wt/vol) sucrose. The next day, the brain was sectioned at 25-μm thickness with a cryostat, and the sections collected on ColorFrost Plus slides (Fisher Scientific) and air-dried overnight at 37 °C. Biocytin was revealed by first rinsing the sections three times for 10 min and incubating them for 30 min in PBS (TBMBS for DA immunofluorescence) containing streptavidin-Alexa Fluor 594, 488, or 350 (1:200, Life Technologies S-11227, S-11223, S-11249), depending on the color needs. The sections were then rinsed three times for 10 min with PBS (or TBMBS) and then processed for immunofluorescence.

Anatomical Tracing and Histology in Rats. Neuronal tracing was carried out by injecting transgenic rats with the Cre-dependent virus AAV-EF1a-DIO-EYFP (titer 1.5–4 × 10^{12} particles per milliliter; serotype AAV5, University of North Carolina Vector Core). Injections followed standard stereotaxic procedures. Small burr holes were drilled either over the PPN (AP −7.8; ML ± 2.0 mm relative to bregma), or the striatum (AP + 1.3; ML ± 2.4). A custom-made 31-gauge infuser (Hamilton Company) connected to a 10-μL Hamilton syringe was locked into a syringe pump (Harvard Apparatus). At the appropriate depth (DV −7.6 mm for PPN, DV −4.5 for striatum, millimeter from skull), 0.3–0.5 μL of virus was delivered at a rate of 0.1 μL/min. The needle was left in place for 5 min before being slowly removed. Following injections, the scalp was sutured and antibiotic ointment applied.

Conventional tracers were used in eight wild-type rats following the same injection procedure. Six rats were injected with both Fast blue [Dr. Numa Dancause, Department of Neurosciences, Université de Montréal, Montréal; 2% (vol/vol) in distilled water] in the striatum and TRDA [MW 10000, 5% (wt/vol) in 0.9% saline] in the PPN. Two other rats received injections of Fast blue in the PPN.

After a waiting period for tracer transport (10 d) or viral expression (6 wk), rats were anesthetized with sodium pentobarbital (100 mg/kg, i.p.) and transcardially perfused with cold PBS followed by 10% (wt/vol) buffered formalin solution (Sigma-Aldrich HT501128). Brains were stored in formalin for 24 h and then transferred to 30% (wt/vol) sucrose in PB until processed. Brains were then snap-frozen in methylbutane at −45 °C and sectioned transversely on a cryostat at 40-μm thickness. The sections were collected in cold PBS, transferred into a cryoprotective solution, and stored at −20 °C until processed for immunofluorescence.

Immunofluorescence in Salamander Brain Tissue. Immunofluorescence against ChAT and TH were carried out simultaneously, based on previous studies (5, 7, 22). All steps were carried out at room temperature unless mentioned otherwise. The sections were first rinsed three times for 10 min with PBS and incubated for 60 min in PBS containing 0.3% Triton X-100 and 5% (vol/vol) normal horse serum (PBSH). The sections were then incubated overnight at 4 °C in PBSH containing the primary antibodies [goat anti-ChAT, Millipore AB144P, lot NG1780580 (1:100); rabbit anti-TH, Millipore AB152, lot 2392225 (1:400)]. The next day, the sections were rinsed three times for 10 min in PBS and incubated for 60 min in PBSH containing the appropriate two secondary antibodies [donkey anti-goat Alexa Fluor 488, Invitrogen A11055 (1:200); donkey anti-rabbit Alexa Fluor 594, Invitrogen A21207 (1:400)]. The sections were then rinsed three times for 10 min with PBS and cover-slipped with Vectashield (H1000, Vector Laboratories). ChAT and TH protocols were also carried out separately without any observable differences in labeling. In the case of triple labeling with two tracers (see above) and TH immunofluorescence, the secondary antibody was a goat anti-rabbit Alexa Fluor 488 (Invitrogen A11008; 1:400). No labeling occurred when the primary antibodies were left out of the procedures. TH immunofluorescence was used to visualize DA neurons, based on studies in salamanders (28, 62). The presence of DA was examined with DA immunofluorescence, in which case TBMBS was used as buffer with 0.5% Triton X-100 and 5% (vol/vol) normal goat serum. The antibodies were a mouse anti-DA (Millipore MAB5300, clone K56A, lot NG1900311; 1:400) and a goat anti-mouse DyLight 594 (Jackson ImmunoResearch 115–515-146; 1:200). All other steps were as described for ChAT and TH.

Immunofluorescence on Rat Brain Tissue. Immunofluorescence against TH or the DAT were each combined with ChAT immunofluorescence. All steps were carried out at room temperature unless otherwise stated. The sections were first rinsed three times 10 min with PBS and incubated for 60 min in a solution of PBS containing 5% (vol/vol) normal goat serum and 0.3% Triton X-100 (PBSG). They were then transferred at 4 °C for 72 h into PBSG containing 0.05% sodium azide and antibodies against TH and ChAT or DAT and ChAT [rabbit anti-TH, Millipore AB152, lot 2392225 (1:1,500); mouse anti-ChAT, clone 1E6, LifeSpan LS-C41821, lot 636741 (1:400); rabbit anti-DAT, Millipore AB1591P, lot 2519289 (1:200)]. The sections were then rinsed three times for 10 min with PBS and transferred for 4 h into PBSG containing the appropriate secondary antibodies [goat anti-rabbit Alexa Fluor 594, Invitrogen A11012 (1:500); goat anti-mouse Alexa Fluor 488, Invitrogen A11001 (1:400)]. The sections were then rinsed three times for 10 min with PBS, mounted on slides and cover-slipped with Vectashield. Consistent with the information provided by the manufacturer of the anti-DAT antibody (Millipore), we found that a 5-min digestion of the tissue (trypsin 1:10, Digest-All kit, ThermoFisher 00–3006) before DAT immunofluorescence greatly increased the intensity of labeling and the number of detectable fibers. ChAT, DAT, and TH immunofluorescence were also carried out separately without any observable differences in labeling. No labeling occurred when the primary antibodies were left out of the procedures.

Immunofluorescence on Human Brain Tissue. The PPN parasagittal sections from one postmortem human brain were first processed for 20 min in citrate buffer (10 mM, pH 6) at 100 °C.

Immunofluorescence against ChAT and DAT or ChAT and TH were combined. All steps were carried out at room temperature unless otherwise stated. The sections were first rinsed three times for 10 min with PBS followed by a 1-h incubation in PBS containing 0.5% Triton X-100, 2% (vol/vol) normal horse serum, and 2% (vol/vol) normal rabbit serum (PBSHR for ChAT and DAT), or in PBS containing 0.5% Triton X-100, 2% (vol/vol) normal horse serum and 2% (vol/vol) normal donkey serum (PBSHD for ChAT and TH). The sections were then transferred for 48 h at 4 °C into PBSHR or PBSHD containing the ChAT and DAT or ChAT and TH antibodies, respectively [goat anti-ChAT, Millipore AB144P, lot 2500411 (1:20); rat anti-DAT, clone DAT-Nt, Millipore MAB369, lot 2567061 (1:1,000); mouse anti-TH, Immunostar 22941, lot 1241002 (1:500)]. The sections were then rinsed three times for 10 min with PBS followed by a 2-h incubation with the secondary antibodies diluted in the same solutions as the primary antibodies [biotinylated horse anti-goat, Vector (1:1,000); rabbit anti-rat Alexa Fluor 594, Invitrogen (1:200); donkey anti-mouse Texas Red, Jackson Immunoresearch 715–075-150 (1:200)]. The sections were again rinsed three times for 10 min with PBS followed by incubation in PBS containing streptavidin-Alexa Fluor 405 (Jackson Immunoresearch 016–470-084; 1:200). The sections were then rinsed three times for 10 min with PBS, mounted on chrome-alum slides, air-dried, treated for autofluorescence (Millipore 2160), and covers-lipped (Dako S3023).

Selection of the Primary Antibodies. The AB144P ChAT antibody was used here on salamander, rat, and human tissue. It is widely used to label cholinergic neurons in many species, including salamanders (5, 7, 59), lampreys (36, 63, 64), and human (65). Alternatively, the LS-C41821 ChAT antibody was also used on rat tissue because of a better signal-to-noise ratio. Characterized by Crawford et al. (66), the LS-C41821 ChAT antibody is routinely used to label cholinergic neurons in the rat brain (67, 68). The labeling obtained with this antibody was very similar to that obtained with AB144P.

The AB152 TH antibody was used here on salamander and rat tissue. It has been widely used in lampreys, salamanders, rats, and human to label DA neurons (manufacturer's information) (22, 28, 69–73). The 22941 TH antibody was used here on human tissue based on its successful use by Parent et al. (74).

To confirm the dopaminergic nature of the TH labeling, antibodies against DA (for salamander) or DAT (for rat and human) were used. The high specificity of the MAB5300 DA antibody was tested by the manufacturer, and its pattern of labeling has been found to be very similar to that obtained with other DA antibodies in lampreys (22, 75, 76) and salamanders (28). The MAB369 DAT antibody was used here on rat and human tissue based on previous studies (77, 78). Alternatively, the AB1591P DAT antibody was used

on rat tissue with very similar results. This is supported by a recent study in the rat, where the two antibodies were shown to selectively label dopaminergic neurons and terminals, and produce very similar patterns of labeling (79).

Microscopy and Photography for Immunofluorescence. Salamander and rat sections were observed and photographed using an E600 epifluorescence microscope equipped with a DXM1200 camera (Nikon). For some rat sections and all human material, a confocal microscope was used (FV1000, Olympus, for rat; LSM 700, Zeiss, for human). Merging digital photomicrographs and adjusting levels of contrast was done in Photoshop CS5 (Adobe).

Calcium Imaging in the Salamander. Based on previous studies (4, 7, 50, 80), the reticulospinal (RS) neurons were retrogradely labeled with the calcium (Ca^{2+}) indicator Ca^{2+} green-dextran amines (MW 3000, Invitrogen C-6765) injected as crystals at the level of the first spinal segment, immediately after a complete transection. The preparation was then transferred for 18–24 h in a chamber perfused with cooled (8–10 °C), oxygenated Ringer's solution to allow the tracer to migrate to fill the RS cell bodies. The next day, a transverse section was performed rostral to the PT to eliminate all inputs from more rostral areas and a midsagittal section was performed at the level of the dorsal diencephalon and mesencephalon to provide access to the PT and MLR. The preparation was then pinned down to the bottom of a recording chamber perfused with cooled (8–10 °C), oxygenated Ringer's solution (4 mL/min). Fluorescence recordings were performed with a fluorescence microscope (Olympus BX50WI) equipped with a custom LED light source. The RS cells of the mRN were easily identified under the microscope (7, 60, 61). An optimal focal plane was chosen for imaging RS cells in the mRN. To measure the change in fluorescence, regions of interest were manually delineated around the RS cell bodies labeled with the Ca^{2+} dye. Ca^{2+} responses of RS neurons to PT stimulation were acquired at a rate of 10 Hz using MicroManager coupled with a with a pco.edge sCMOS camera (PCO tech). The Ca^{2+} responses were expressed as relative changes in fluorescence ($\Delta F/F$). The baseline was defined as the averaged fluorescence before stimulation. Data analysis was carried out using ImageJ, Clampfit (Molecular Devices) and Matlab (Mathworks).

Electrical Stimulation. In salamanders, homemade glass-coated tungsten microelectrodes (0.5–3.5 MΩ with a 10- to 30-μm exposed tip) were used with a Grass Instrument S88 stimulator coupled to a Grass PSIU6 photoelectric isolation unit for controlling the stimulation intensity (Astro Med), as described elsewhere (e.g., refs. 7 and 22). Square pulses (2-ms duration) were applied at 5 Hz for 10 s. A pause of 3 to 5 min was allowed between two stimulations. The stimulation intensities ranged from 1 to 15 μA. The stimulation site was chosen based on a previous study (62) and gathered data from the present study.

In rats, a bipolar-stimulating electrode (0.20-mm diameter; Plastics One), with poles separated by 0.5–1 mm, was lowered into the right SNc/RRF region (AP −6.4, ML +1.7, −7.5 mm DV from brain surface). A chlorinated Ag/AgCl reference electrode was placed in left forebrain and secured with a single screw and dental acrylic. Trains of electrical stimulation (60 Hz, 5-ms pulses, 60 pulses, 120 μA) were applied each 5 min to the SNc/RRF region. In both salamander and rat experiments, the location of the stimulation site was verified histologically by performing an electrolytic lesion in situ at the end of the experiment (5 s, DC current, 10 μA) followed by TH immunofluorescence.

Voltammetry Recordings. Changes in DA concentration were measured using fast-scan cyclic voltammetry with glass-insulated, nafion-coated, carbon-fiber microelectrodes (22, 81). The voltage of the recording electrode was held at −0.4 V and ramped in a triangular fashion (−0.4 to +1.3 to −0.4 V; 400 V/s; "scan") at 60 Hz during a 30-min equilibration period during which time no data were collected. During data collection, scans were applied at 10 Hz. Electroactive species within this voltage range oxidize and reduce at different points along the voltage scan and can be identified on the basis of their background-subtracted current by voltage (cyclic voltammogram; CV) plots (22, 81). DA was identified by its traditional oxidation peak (~0.6 V) as in lampreys (22) and rats (81, 82). H_2O_2 was identified by its distinct, well-defined oxidation peak (~1.2 V), as previously reported (83).

In salamanders, the recording electrode was placed in the LDT (5, 7), whereas in rats it was positioned over the PPN (AP −7.8, ML +2.0) and slowly lowered into place (~−7.0–7.5 mm from brain surface) (2). A chlorinated Ag/AgCl reference electrode was placed in the bath for in vitro salamander recordings or in the forebrain for in vivo rat recordings. Following the equilibration period described above, we first sought to verify that the recording location supported DA release. To do so, trains of stimulation were delivered to the SNc/RRF region in rats or PT in salamanders, and the resultant changes in current at each potential of the electrode were examined. If this failed to evoke DA release, the recording electrode was advanced 50–100 μm and the process was repeated. Once a stable release site was confirmed, the experiment began. To verify histologically the location of the recording site, electrolytic lesion (5 s, DC current, 10 μA) was performed through the recording electrode in situ at the end of the experiment. Quantifications of the changes in DA release were performed by calculating the area under the curve (in nM × s) from the beginning of the response to the return to baseline using the area calculation script in Clampfit (Molecular Devices). In the text, the normalized areas are expressed in percent of baseline.

Drugs. D-Glutamate (Sigma-Aldrich G1001, 5 mM in Ringer's solution) was microinjected locally in the PT of salamanders through a glass micropipette (tip diameter 4–6 μm) by applying trains (10 s, 2 Hz) of pressure pulses (5–20 psi) of various durations (50–200 ms) with a Picospritzer (Parker Hannifin) (e.g., refs. 4, 7, 22, 84). Fast green was added to the solution for visualizing the injection site (e.g., refs. 7, 22, 37, 50, 58). The number of moles of ejected glutamate was estimated by measuring the volume of a droplet ejected in the air following a single pressure pulse multiplied by the number of pressure pulses (e.g., refs. 7, 22, 36, 84). In anesthetized rats, amphetamine (in 0.9% saline; Sigma) was injected intraperitoneally at 5 mg/kg.

Statistics. Data in the text are presented as the mean ± SEM. Statistical analyses were performed with Sigma Plot 11.0 (Systat). Two-tailed paired Student's *t* tests were used for comparing means between two groups. Correlations between variables were calculated using the Pearson Product Moment Correlation test. Statistical differences were considered to be significant when $P < 0.05$. All figures were designed with Illustrator CS5 software (Adobe Systems).

ACKNOWLEDGMENTS. We thank Danielle Veilleux and Marie-Josée Wallman for technical assistance; Frédéric Bernard for help with the graphics; and Dr. Numa Dancause for the generous gift of the Fast blue tracer. This work was supported by the Canadian Institutes of Health Research (15129); the Fonds de la Recherche en Santé du Québec (Groupe de Recherche sur le Système Nerveux Central, GRSNC, 5249); Natural Sciences and Engineering Research Council of Canada Grant 217435 (to R.D.); Great Lakes Fishery Commission Grants 54011 and 54021 (to R.D.); a fellowship from the Fonds de la Recherche en Santé du Québec (to D.R.); and the GRSNC Jasper fellowship (to D.R.).

1. Shik ML, Severin FV, Orlovskiĭ GN (1966) [Control of walking and running by means of electric stimulation of the midbrain]. *Biofizika* 11(4):659–666. Russian.
2. Garcia-Rill E, Houser CR, Skinner RD, Smith W, Woodward DJ (1987) Locomotion-inducing sites in the vicinity of the pedunculopontine nucleus. *Brain Res Bull* 18(6):731–738.
3. Sirota MG, Di Prisco GV, Dubuc R (2000) Stimulation of the mesencephalic locomotor region elicits controlled swimming in semi-intact lampreys. *Eur J Neurosci* 12(11):4081–4092.
4. Brocard F, et al. (2010) The transformation of a unilateral locomotor command into a symmetrical bilateral activation in the brainstem. *J Neurosci* 30(2):523–533.
5. Cabelguen JM, Bourcier-Lucas C, Dubuc R (2003) Bimodal locomotion elicited by electrical stimulation of the midbrain in the salamander *Notophthalmus viridescens*. *J Neurosci* 23(6):2434–2439.
6. Bachmann LC, et al. (2013) Deep brain stimulation of the midbrain locomotor region improves paretic hindlimb function after spinal cord injury in rats. *Sci Transl Med* 5(208):208ra146.
7. Ryczko D, Auclair F, Cabelguen JM, Dubuc R (2016) The mesencephalic locomotor region sends a bilateral glutamatergic drive to hindbrain reticulospinal neurons in a tetrapod. *J Comp Neurol* 524(7):1361–1383.
8. Ryczko D, Dubuc R (2013) The multifunctional mesencephalic locomotor region. *Curr Pharm Des* 19(24):4448–4470.
9. Pombal MA, El Manira A, Grillner S (1997) Afferents of the lamprey striatum with special reference to the dopaminergic system: A combined tracing and imunohistochemical study. *J Comp Neurol* 386(1):71–91.
10. Pombal MA, El Manira A, Grillner S (1997) Organization of the lamprey striatum—Transmitters and projections. *Brain Res* 766(1-2):249–254.
11. Kravitz AV, et al. (2010) Regulation of parkinsonian motor behaviours by optogenetic control of basal ganglia circuitry. *Nature* 466(7306):622–626.
12. Grillner S, Robertson B, Stephenson-Jones M (2013) The evolutionary origin of the vertebrate basal ganglia and its role in action selection. *J Physiol* 591(22):5425–5431.
13. Wullimann MF (2014) Ancestry of basal ganglia circuits: New evidence in teleosts. *J Comp Neurol* 522(9):2013–2018.
14. Wullimann MF (2011) Basal ganglia: Insights into origins from lamprey brains. *Curr Biol* 21(13):R497–R500.
15. Marín O, Smeets WJ, González A (1997) Basal ganglia organization in amphibians: Catecholaminergic innervation of the striatum and the nucleus accumbens. *J Comp Neurol* 378(1):50–69.
16. Puelles L, Verney C (1998) Early neuromeric distribution of tyrosine-hydroxylase-immunoreactive neurons in human embryos. *J Comp Neurol* 394(3):283–308.

17. Rink E, Wullimann MF (2001) The teleostean (zebrafish) dopaminergic system ascending to the subpallium (striatum) is located in the basal diencephalon (posterior tuberculum). *Brain Res* 889(1-2):316–330.
18. Blin M, Norton W, Bally-Cuif L, Vernier P (2008) NR4A2 controls the differentiation of selective dopaminergic nuclei in the zebrafish brain. *Mol Cell Neurosci* 39(4):592–604.
19. Smeets WJ, Marín O, González A (2000) Evolution of the basal ganglia: New perspectives through a comparative approach. *J Anat* 196(Pt 4):501–517.
20. Yamamoto K, Vernier P (2011) The evolution of dopamine systems in chordates. *Front Neuroanat* 5:21.
21. Filippi A, Mueller T, Driever W (2014) Vglut2 and gad expression reveal distinct patterns of dual GABAergic versus glutamatergic cotransmitter phenotypes of dopaminergic and noradrenergic neurons in the zebrafish brain. *J Comp Neurol* 522(9):2019–2037.
22. Ryczko D, et al. (2013) Forebrain dopamine neurons project down to a brainstem region controlling locomotion. *Proc Natl Acad Sci USA* 110(34):E3235–E3242.
23. Pérez-Fernández J, Stephenson-Jones M, Suryanarayana SM, Robertson B, Grillner S (2014) Evolutionarily conserved organization of the dopaminergic system in lamprey: SNc/VTA afferent and efferent connectivity and D2 receptor expression. *J Comp Neurol* 522(17):3775–3794.
24. Beckstead RM, Domesick VB, Nauta WJ (1979) Efferent connections of the substantia nigra and ventral tegmental area in the rat. *Brain Res* 175(2):191–217.
25. Semba K, Fibiger HC (1992) Afferent connections of the laterodorsal and the pedunculopontine tegmental nuclei in the rat: A retro- and antero-grade transport and immunohistochemical study. *J Comp Neurol* 323(3):387–410.
26. Scarnati E, Proia A, Di Loreto S, Pacitti C (1987) The reciprocal electrophysiological influence between the nucleus tegmenti pedunculopontinus and the substantia nigra in normal and decorticated rats. *Brain Res* 423(1-2):116–124.
27. Rolland AS, et al. (2009) Evidence for a dopaminergic innervation of the pedunculopontine nucleus in monkeys, and its drastic reduction after MPTP intoxication. *J Neurochem* 110(4):1321–1329.
28. Gonzalez A, Smeets WJ (1991) Comparative analysis of dopamine and tyrosine hydroxylase immunoreactivities in the brain of two amphibians, the anuran *Rana ridibunda* and the urodele *Pleurodeles waltlii*. *J Comp Neurol* 303(3):457–477.
29. Yamamoto K, Ruuskanen JO, Wullimann MF, Vernier P (2010) Two tyrosine hydroxylase genes in vertebrates. New dopaminergic territories revealed in the zebrafish brain. *Mol Cell Neurosci* 43(4):394–402.
30. Witten IB, et al. (2011) Recombinase-driver rat lines: Tools, techniques, and optogenetic application to dopamine-mediated reinforcement. *Neuron* 72(5):721–733.
31. Aschauer DF, Kreuz S, Rumpel S (2013) Analysis of transduction efficiency, tropism and axonal transport of AAV serotypes 1, 2, 5, 6, 8 and 9 in the mouse brain. *PLoS One* 8(9):e76310.
32. Gerfen CR, Staines WA, Arbuthnott GW, Fibiger HC (1982) Crossed connections of the substantia nigra in the rat. *J Comp Neurol* 207(3):283–303.
33. Edley SM, Graybiel AM (1983) The afferent and efferent connections of the feline nucleus tegmenti pedunculopontinus, pars compacta. *J Comp Neurol* 217(2):187–215.
34. Masdeu JC, Alampur U, Cavaliere R, Tavoulareas G (1994) Astasia and gait failure with damage of the pontomesencephalic locomotor region. *Ann Neurol* 35(5):619–621.
35. Karachi C, et al. (2010) Cholinergic mesencephalic neurons are involved in gait and postural disorders in Parkinson disease. *J Clin Invest* 120(8):2745–2754.
36. Le Ray D, et al. (2003) Nicotinic activation of reticulospinal cells involved in the control of swimming in lampreys. *Eur J Neurosci* 17(1):137–148.
37. Brocard F, Dubuc R (2003) Differential contribution of reticulospinal cells to the control of locomotion induced by the mesencephalic locomotor region. *J Neurophysiol* 90(3): 1714–1727.
38. Lee AM, et al. (2014) Identification of a brainstem circuit regulating visual cortical state in parallel with locomotion. *Neuron* 83(2):455–466.
39. Franzoni MF, et al. (1986) Organization of tyrosine-hydroxylase immunopositive neurons in the brain of the crested newt, *Triturus cristatus carnifex*. *J Comp Neurol* 251(1):121–134.
40. Pombal MA, Puelles L (1999) Prosomeric map of the lamprey forebrain based on calretinin immunocytochemistry, Nissl stain, and ancillary markers. *J Comp Neurol* 414(3):391–422.
41. Barreiro-Iglesias A, Villar-Cerviño V, Anadón R, Rodicio MC (2008) Descending brain-spinal cord projections in a primitive vertebrate, the lamprey: Cerebrospinal fluid-contacting and dopaminergic neurons. *J Comp Neurol* 511(6):711–723.
42. Tay TL, Ronneberger O, Ryu S, Nitschke R, Driever W (2011) Comprehensive catecholaminergic projectome analysis reveals single-neuron integration of zebrafish ascending and descending dopaminergic systems. *Nat Commun* 2:171.
43. Koblinger K, et al. (2014) Characterization of A11 neurons projecting to the spinal cord of mice. *PLoS One* 9(10):e109636.
44. Skagerberg G, Lindvall O (1985) Organization of diencephalic dopamine neurones projecting to the spinal cord in the rat. *Brain Res* 342(2):340–351.
45. Barraud Q, et al. (2010) Neuroanatomical study of the A11 diencephalospinal pathway in the non-human primate. *PLoS One* 5(10):e13306.
46. Lorang D, Amara SG, Simerly RB (1994) Cell-type-specific expression of catecholamine transporters in the rat brain. *J Neurosci* 14(8):4903–4914.
47. Ciliax BJ, et al. (1999) Immunocytochemical localization of the dopamine transporter in human brain. *J Comp Neurol* 409(1):38–56.
48. Sharples SA, Koblinger K, Humphreys JM, Whelan PJ (2014) Dopamine: A parallel pathway for the modulation of spinal locomotor networks. *Front Neural Circuits* 8:55.
49. Gerin C, Becquet D, Privat A (1995) Direct evidence for the link between monoaminergic descending pathways and motor activity. I. A study with microdialysis probes implanted in the ventral funiculus of the spinal cord. *Brain Res* 704(2):191–201.
50. Derjean D, et al. (2010) A novel neural substrate for the transformation of olfactory inputs into motor output. *PLoS Biol* 8(12):e1000567.
51. Morales M, Root DH (2014) Glutamate neurons within the midbrain dopamine regions. *Neuroscience* 282C:60–68.
52. Cepeda C, Buchwald NA, Levine MS (1993) Neuromodulatory actions of dopamine in the neostriatum are dependent upon the excitatory amino acid receptor subtypes activated. *Proc Natl Acad Sci USA* 90(20):9576–9580.
53. Tseng KY, O'Donnell P (2004) Dopamine-glutamate interactions controlling prefrontal cortical pyramidal cell excitability involve multiple signaling mechanisms. *J Neurosci* 24(22):5131–5139.
54. Schultz W, Dayan P, Montague PR (1997) A neural substrate of prediction and reward. *Science* 275(5306):1593–1599.
55. McCutcheon JE, et al. (2014) Optical suppression of drug-evoked phasic dopamine release. *Front Neural Circuits* 8:114.
56. Paxinos G, Watson C (2005) *The Rat Brain in Stereotaxic Coordinates* (Academic, San Diego, CA), 4th Ed.
57. Gariépy JF, et al. (2012) Specific neural substrate linking respiration to locomotion. *Proc Natl Acad Sci USA* 109(2):E84–E92.
58. Gariépy JF, et al. (2012) Bilateral connectivity in the brainstem respiratory networks of lampreys. *J Comp Neurol* 520(7):1442–1456.
59. Marín O, Smeets WJ, González A (1997) Distribution of choline acetyltransferase immunoreactivity in the brain of anuran (*Rana perezi*, *Xenopus laevis*) and urodele (*Pleurodeles waltl*) amphibians. *J Comp Neurol* 382(4):499–534.
60. Naujoks-Manteuffel C, Manteuffel G (1988) Origins of descending projections to the medulla oblongata and rostral medulla spinalis in the urodele *Salamandra salamandra* (amphibia). *J Comp Neurol* 273(2):187–206.
61. Sánchez-Camacho C, Marín O, Ten Donkelaar HJ, González A (2001) Descending supraspinal pathways in amphibians. I. A dextran amine tracing study of their cells of origin. *J Comp Neurol* 434(2):186–208.
62. Parish CL, Beljajeva A, Arenas E, Simon A (2007) Midbrain dopaminergic neurogenesis and behavioural recovery in a salamander lesion-induced regeneration model. *Development* 134(15):2881–2887.
63. Pombal MA, Marín O, González A (2001) Distribution of choline acetyltransferase-immunoreactive structures in the lamprey brain. *J Comp Neurol* 431(1):105–126.
64. Quinlan KA, Buchanan JT (2008) Cellular and synaptic actions of acetylcholine in the lamprey spinal cord. *J Neurophysiol* 100(2):1020–1031.
65. Massouh M, Wallman MJ, Pourcher E, Parent A (2008) The fate of the large striatal interneurons expressing calretinin in Huntington's disease. *Neurosci Res* 62(4):216–224.
66. Crawford GD, Correa L, Salvaterra PM (1982) Interaction of monoclonal antibodies with mammalian choline acetyltransferase. *Proc Natl Acad Sci USA* 79(22):7031–7035.
67. Wisman LA, Sahin G, Maingay M, Leanza G, Kirik D (2008) Functional convergence of dopaminergic and cholinergic input is critical for hippocampus-dependent working memory. *J Neurosci* 28(31):7797–7807.
68. Yang Z, You Y, Levison SW (2008) Neonatal hypoxic/ischemic brain injury induces production of calretinin-expressing interneurons in the striatum. *J Comp Neurol* 511(1):19–33.
69. López JM, Moreno N, Morona R, Muñoz M, González A (2005) Colocalization of nitric oxide synthase and monoamines in neurons of the amphibian brain. *Brain Res Bull* 66(4-6):555–559.
70. Villar-Cerviño V, et al. (2006) Presence of glutamate, glycine, and gamma-aminobutyric acid in the retina of the larval sea lamprey: Comparative immunohistochemical study of classical neurotransmitters in larval and postmetamorphic retinas. *J Comp Neurol* 499(5):810–827.
71. Barreiro-Iglesias A, Villar-Cerviño V, Villar-Cheda B, Anadón R, Rodicio MC (2008) Neurochemical characterization of sea lamprey taste buds and afferent gustatory fibers: Presence of serotonin, calretinin, and CGRP immunoreactivity in taste bud biciliated cells of the earliest vertebrates. *J Comp Neurol* 511(4):438–453.
72. Robertson B, et al. (2012) The dopamine D2 receptor gene in lamprey, its expression in the striatum and cellular effects of D2 receptor activation. *PLoS One* 7(4):e35642.
73. McCutcheon JE, et al. (2012) Dopamine neurons in the ventral tegmental area fire faster in adolescent rats than in adults. *J Neurophysiol* 108(6):1620–1630.
74. Parent M, Bédard C, Pourcher E (2013) Dopaminergic innervation of the human subventricular zone: A comparison between Huntington's chorea and Parkinson's disease. *Am J Neurodegener Dis* 2(3):221–227.
75. Pierre J, Mahouche M, Suderevskaya EI, Repérant J, Ward R (1997) Immunocytochemical localization of dopamine and its synthetic enzymes in the central nervous system of the lamprey *Lampetra fluviatilis*. *J Comp Neurol* 380(1):119–135.
76. Abalo XM, Villar-Cheda B, Anadón R, Rodicio MC (2005) Development of the dopamine-immunoreactive system in the central nervous system of the sea lamprey. *Brain Res Bull* 66(4-6):560–564.
77. Ciliax BJ, et al. (1995) The dopamine transporter: Immunochemical characterization and localization in brain. *J Neurosci* 15(3 Pt 1):1714–1723.
78. Huot P, Lévesque M, Parent A (2007) The fate of striatal dopaminergic neurons in Parkinson's disease and Huntington's chorea. *Brain* 130(Pt 1):222–232.
79. Afonso-Oramas D, et al. (2009) Dopamine transporter glycosylation correlates with the vulnerability of midbrain dopaminergic cells in Parkinson's disease. *Neurobiol Dis* 36(3):494–508.
80. Di Prisco GV, Pearlstein E, Robitaille R, Dubuc R (1997) Role of sensory-evoked NMDA plateau potentials in the initiation of locomotion. *Science* 278(5340):1122–1125.
81. Roitman MF, Wheeler RA, Wightman RM, Carelli RM (2008) Real-time chemical responses in the nucleus accumbens differentiate rewarding and aversive stimuli. *Nat Neurosci* 11(12):1376–1377.
82. Sinkala E, et al. (2012) Electrode calibration with a microfluidic flow cell for fast-scan cyclic voltammetry. *Lab Chip* 12(13):2403–2408.
83. Sanford AL, et al. (2010) Voltammetric detection of hydrogen peroxide at carbon fiber microelectrodes. *Anal Chem* 82(12):5205–5210.
84. Brocard F, Bardy C, Dubuc R (2005) Modulatory effect of substance P to the brain stem locomotor command in lampreys. *J Neurophysiol* 93(4):2127–2141.